Published in final edited form as:
Biomaterials. 2011 December ; 32(34): 8927–8937. doi:10.1016/j.biomaterials.2011.08.027.

Effect of initial cell seeding density on 3D-engineered silk fibroin scaffolds for articular cartilage tissue engineering

Sarmistha Talukdar[a,#], **Quynhhoa T. Nguyen**[b,#], **Albert C. Chen**[b], **Robert L. Sah**[b,*], and **Subhas C. Kundu**[a,*]

[a]Department of Biotechnology, Indian Institute of Technology, Kharagpur-721302, India

[b]Department of Bioengineering, University of California-San Diego, La Jolla, CA, 92093 USA

Abstract

The repair of articular cartilage defects poses a continuing challenge. Cartilage tissue engineering through the culture of chondrocytes seeded in 3D porous scaffolds has the potential for generating constructs that repair successfully. It also provides a platform to study scaffold-cell and cell-cell interactions. The scaffold affects the growth and morphology of cells growing on it, and concomitantly, cells affect the properties of the resultant tissue construct. Silk fibroin protein from *Antheraea mylitta*, a non-mulberry Indian tropical tasar silkworm, is a potential biomaterial for diverse applications due to its widespread versatility as a mechanically robust, biocompatible, tissue engineering material. Analysis of silk fibroin scaffolds seeded with varying initial densities (25, 50 and 100 million cells/ml) and cultured for 2 weeks showed that thickness and wet weight increased by 60–70% for the highest cell density, and DNA, GAG and collagen content of the cartilaginous constructs increased with increasing cell density. Mechanical characterization of the constructs elucidated that the highest density constructs had compressive stiffness and modulus 4–5 times that of cell-free scaffolds. The present results indicate the importance of cell seeding density in the rapid formation of a functional cartilaginous tissue.

Keywords

Silk fibroin; chondrocyte; 3D scaffold; ECM; articular cartilage; tissue engineering

1. INTRODUCTION

In spite of availability of surgical and non surgical procedures, the repair and regeneration of articular cartilage lesions remains an obdurate problem. Adult articular cartilage possesses limited self-repair capacity, whether damage is caused by developmental abnormalities, trauma, or aging-related degeneration like osteoarthritis. Once damaged, the propensity to regenerate is limited by its avascular nature and lack of sufficient reparative cells. The low cell to matrix ratio of cartilage is one limiting factor to the poor reparative property of the tissue [1].

[*]Corresponding authors: Professor Robert L. Sah, Telephone: (858) 534-0821, Fax: (858) 822-1614, rsah@ucsd.edu (Robert L Sah). Professor S. C. Kundu, Telephone: +91-3222- 283764, Fax: +91-3222-278433, kundu@hijli.iitkgp.ernet.in (S. C. Kundu).
[#]Equal Contributions

Recent experimental and clinical studies of cartilage repair have examined a number of cell-based tissue-engineering methods for cartilage repair and regeneration [2–4]. There is a need for fabricating repair material and delivering it to the site of damage. Scaffold-based 3D extracellular matrices (ECM) are widely used in tissue engineering to support, reinforce and in some cases organize regenerative tissues and to deliver therapeutic cells [5, 4]. Such 3D scaffolds create a microenvironment with cell-cell interactions and expressions of different cellular functions [6]. Several natural biomaterials, such as collagen [7], hyaluronan [8], fibrin glue [9], alginate [3], agarose [10], chitosan [11, 12], cellulose [13], mulberry silk [14, 15] as well as synthetic biomaterials such as PLA [16], PLGA [17, 18], poly(glycerol sebacate) [19] have extensively been used in cartilage tissue engineering. *In vitro* cartilage tissue engineering using chondrocytes and three-dimensional (3D) porous scaffolds can facilitate an understanding of cartilage regeneration as well as provide materials for the repair of cartilage damage.

A major challenge for cartilage repair is finding a material that can simultaneously facilitate cell division and ECM, and biodegrade slowly until repair is complete. Natural fibrous silk fibroin (SF) protein, is used as biomaterial for tissue engineering in the form of films, membranes, gels, sponges, powders, and scaffolds [20, 21]. Mulberry SF protein acts as a supporting matrix for a variety of cell types because of its conducive surface chemistry, supporting cell attachment and proliferation. It has been used to study several cells [20] including chondrocytes [22, 14]. Silk from *Antheraea mylitta*, a non-mulberry silkworm is also a potential biomaterial for diverse applications due to its widespread versatility as a mechanically robust, biocompatible, slowly biodegradable, and tissue engineering material [23–25].

Cartilage tissue engineering has been carried out with a variety of initial densities for seeding biomaterials in order to form cartilage tissue constructs with a variety of properties. Cell seeding density (0 – 120 million cells/ml) has considerable effects on the developing composition, structure, and biomechanical function of cartilage constructs [26–30]. Significant differences were noticed in morphology, total collagen, GAG content, and permeability of the constructs [30–32]. While cell seeding density may increase GAG accumulation [31], high seeding density might also limit nutrient uptake [32]. It is thus of interest to investigate the effect of chondrocyte cell seeding density on both biomechanical and biochemical properties of cartilage constructs. In the current study, we examined the effect of cell seeding density with non-mulberry Indian tropical tasar silkworm *A. mylitta* silk fibroin protein scaffolds on the development of *in vitro* cartilaginous constructs. This study examined the growth and proliferation of immature articular chondrocytes on the scaffold material, accumulation of cellular and extracellular matrix components, compressive mechanical properties and associated changes in composition and function.

2. MATERIALS AND METHODS

2.1 Chemicals and antibodies

Sodium dodecyl sulfate (SDS) (Qualigens, Mumbai, India), polyethylene glycol (PEG) 6000 (SRL, Mumbai, India), Tris, EDTA, hydroxyproline, FW 131.1 (trans-4-Hydroxy-L-Proline), Alcian blue, DMBA (p-dimethylaminobenzaldehdye) FW 149.2, Chloramine T hydrate, FW 227.6, citric acid monohydrate, FW 210.1, Dulbecco's Modified Eagle's medium (DMEM), MEM, Non-Essential Amino Acids Solution, L-Proline, L-glutamine, HEPES, ascorbate, pronase type XIV (Sigma-Aldrich, USA), fetal calf serum, trypsin–EDTA, Live dead assay, HBBS (Invitrogen-Gibco, Grand Island, NY), antibiotic-antimycotic, collagenase P (Roche Diagnostics, USA), 1,9-dimethylmethylene blue chloride, glutaraldehyde, (Polysciences Inc, USA), glycine FW 75.07 (Boehringer Mannheim, USA), Sodium chloride FW 58.44, Propanol (1-propanol), FW 60.10, sodium acetate trihydrate,

FW 136.08, sodium hydroxide solid, FW 40.0, glacial acetic acid, FW 60.05, perchloric Acid, 60%, FW 100.46, 2% Sodium Azide (Fisher Scientific, USA), Picogreen, proteinase K (Roche Diagnostics, USA), Vector staining kit, methyl green (Vector Labs) and primary antibodies against bovine Collagen type I and II (Chemicon, USA) were used in the experiments.

2.2. Preparation of 3D Silk Fibroin Scaffolds

Fully mature 5th instar live larvae of Indian tropical tasar silkworm, *Antherarea mylitta* were collected from local silk farms for fibroin protein extraction. The larvae were dissected to extract silk fibroin protein from the posterior silk glands. *A. mylitta* silk fibroin protein was prepared as described in our earlier procedure [33]. Briefly, the glands were washed with double distilled water and finally squeezed with fine forceps to extrude fibroin protein. The extracted protein was solubilized in 1 w/v% sodium dodecyl sulfate (SDS) aqueous solution containing 10 mM Tris (pH 8.0) and 5 mM EDTA at room temperature. Extensive dialysis was carried to remove excess surfactant using dialysis membranes (MWCO 12000) followed by colorimetric estimation of residual SDS concentration. Fibroin concentration was determined by weighing the remaining solid mass after drying at 37°C overnight.

The fibroin solutions with 2 wt%, concentrations were obtained through concentrating the above fibroin solution against PEG. The solution was put into the moulds and then frozen in refrigerator at 20°C for 12 h. The ice/silk composites were then lyophilized leaving a porous matrix. The matrixes were immersed in 70% ethanol for about 1 h to induce crystallization and insolubility in water. The scaffolds were punched with the help of a sterile puncher to a diameter of 6.4 mm. The thickness and wet weight of the scaffolds were noted. The scaffolds were then washed for 1 hour with sterile PBS (pH 7.4) to wash away the residual alcohol, and then conditioned in DMEM for 30 mins.

2.3 Porosity measurements

Non-seeded silk fibroin 3D scaffolds were stained with Hoechst 33342 and analyzed using confocal microscopy. The scaffolds were scanned and analyzed by confocal FV 1000 Advance software v. 4.1 (Olympus). The pore sizes were determined by measuring 50 random pores of the scaffold by Image J software (Wayne Rasband, National Institute of Health, USA).

2.4 Cell isolation from bovine cartilage

Chondrocytes were isolated by sequential enzymatic digestion with pronase and collagenase [34]. Pieces of articular cartilage from the knee joints of two immature bovines were cut, minced and weighed. The cell suspension was rinsed with DMEM, and then passed sequentially through 70 μm and 40 μm pore-size cell sieve (BD Falcon, Unitech, Ireland), and the filtrate centrifuged at 750g for 5 mins at 4°C and rinsed with PBS twice. The isolated chondrocytes were stained with trypan blue, counted, and then diluted to desired concentration.

2.5 Tissue Culture

Prior to culture, the thickness of each 6.4 mm diameter scaffold was measured using a laser micrometer, and volume was calculated. Based on the volume of the scaffold, volume of the stock cell suspension was calculated. Scaffolds were placed in 6-well plates with sterile PBS placed in one of the 6 well plates to maintain humidity. The chondrocytes were seeded on to top of the preconditioned scaffolds in total volume of about 5–13 μl (depending on the volume of the scaffold) at seeding densities of 25 million, 50 million and 100 million cells/

ml (Fig. 1). Scaffolds were incubated for 14d with media changes every other day. Spent medium was collected for biochemical analysis.

2.6 Biochemical analysis

Some 14-day constructs were analyzed biochemically. The construct was weighed wet and solubilized with proteinase K at 60°C overnight. Portions of the digest were analyzed to quantify the mass of sulfated glycosaminoglycan (GAG) [35], hydroxyproline [36], and DNA using PicoGreen [37]. The hydroxyproline content was converted to collagen (COL) content using a mass ratio of collagen to hydroxyproline equal to 7.25 [38]. The molar ratio of cross-link per triple helical collagen molecule was calculated, assuming that the molecular weight of collagen triple helix was 300,000. DNA was converted to cell number using a conversion factor of 7.7 pg DNA/cell [39]. The non-seeded scaffolds did not exhibit any detectable signal with the assays used. The content of individual constituents was calculated as the mass normalized to wet weight (WW). The rest of the samples were then tested for cell viability.

2.7 Chondrocyte Viability

Some constructs were analyzed for dead and living cells. Samples were stained with calcein and ethidium bromide to visualize the population of live and dead cells in the engineered construct after Day 14. Briefly, scaffolds were incubated at 37°C in PBS containing calcein AM and ethidium homodimer-1 (Molecular Probes) for 20min to stain viable and non-viable cells, respectively, and then washed twice in PBS for 10min each. Constructs were sectioned in half to expose a full-thickness plane and imaged by fluorescent microscopy. The percentage of live cells was calculated for each sample from counts of the number of live and dead cells from 3 images at 20× magnification.

2.8 Biomechanical Assessment of Engineered Constructs

Some seeded and non-seeded silk constructs (n=3 each) were analyzed by static and dynamic unconfined compression. In brief, the samples were compressed to 40% and then allowed to relax to equilibrium (2400s or 0.002 MPa/180s). Then, the sample was subjected to a dynamic displacement of 5% amplitude relative to the compressed thickness, at frequencies of f = 0.005, 0.015, 0.05, 0.15, 0.5, 1.5 Hz. From the static equilibrium data, Young's modulus, E, was determined. From the dynamic data, dynamic stiffness amplitude and phase were determined.

2.9 Histology

2.9.1 Alcian Blue staining—To qualitatively analyze proteoglycan content, scaffolds were cryosectioned, fixed, and stained with Alcian Blue. The sections were destained with 3% acetic acid and dehydrated in graded series of alcohol containing 3% acetic acid.

2.9.2 Immunohistochemistry—To qualitatively localize and assess the extent to which the chondrocytes synthesized Type I and Type II collagen, immunohistochemical analysis was performed. Briefly the scaffolds were cryosectioned, fixed, blocked with 2.5% normal horse serum incubated with primary antibodies against bovine Type I or Type II collagen antibodies, then with biotinylated secondary antibody, an assay buffer, and then treated with the substrate until development of color. The sections were counterstained with methyl green.

2.10. Statistical analysis and data presentation

Data are presented as mean ±SEM. Single factor ANOVA and paired one tailed students T-test was done to analyze the significance of the variations in the biochemical content of the

scaffolds and the initial cell seeding density. DNA, cellularity, and dynamic biomechanical data were analyzed by repeated measures ANOVA. Univariate and multivariate linear regression were used to analyze relationships between the constructs' mechanical properties and biochemical content. For data from chondrocyte–seeded constructs, significant relationships were determined using a criterion of $p<0.05$ on regression slopes.

3. RESULTS

3.1 Physical Characteristics of Constructs

The non-seeded silk scaffolds possessed a porous structure throughout (Fig. 2A). Pore sizes were observed to be 150–200 μm. Construct growth was apparent macroscopically. Constructs with the highest cell density became visibly larger and more opaque during culture. Quantitative measures of the construct structural properties including thickness (Fig. 2B) and wet weight (Fig. 2C), confirmed visual observations. After 2 weeks of culture, constructs seeded initially at 25, 50 and 100 million cells/ml had wet weight which was significantly greater than those of non seeded scaffolds ($p<0.05$). The thickness of the seeded scaffolds tended to be higher than that of non seeded scaffolds ($p=0.13$).

3.2 Live/Dead assay

A high proportion of the seeded cells attached to and grew within the scaffold (Fig. 3). Cells were generally spherical/oval in shape. Cells were qualitatively visible throughout the scaffold, irrespective of the initial seeding density. The percentage of live cells was 75–85%. The number of live cells was highest in scaffolds seeded with 100 million cells, followed by 50 and 25 million cells respectively.

3.3. Biochemical analysis of silk fibroin-cartilaginous constructs

3.3.1 DNA content of scaffolds—The DNA content, and deduced cell content (Fig. 4), increased with seeding density ($p<0.001$, ANOVA) and after 14 days of culture ($p<0.001$, ANOVA), with an interaction effect ($p<0.05$, ANOVA). Cellularity increased roughly in proportion with the stepwise increases in the initial seeding density (each $p<0.001$). Compared to the number of cells at day 1, the increase in cells at day 14 was 77%, 56%, and 57% for 25, 50, and 100 million cells/ml seeding densities, respectively. Thus, cell proliferation occurred for all of the seeding conditions during the 14 day culture period.

3.3.2 sGAG content—The sulfated GAG content after 14 days of culture (Fig. 5A) also increased with cell seeding density, both in the construct (ANOVA $p<0.0001$), in the medium (ANOVA $p<0.0001$), and overall (ANOVA $p<0.0001$). GAG increased roughly in proportion with the stepwise increases in the initial seeding density (each $p<0.001$). The increase in GAG content was associated with differences in cell seeding density, as GAG content normalized to DNA content was not different between groups seeded with different numbers of cells (ANOVA, $p=0.30$, Fig. 5B). The percentage of GAG retained within constructs was 66%, 55%, and 56% at the seeding densities of 25, 50, and 100 million cells/ml.

3.3.3. Collagen content—The collagen content after 14 days of culture (Fig. 5C) also increased with increasing cell seeding density (ANOVA $p<0.001$). The scaffolds seeded with 100 million cells/ml had the highest collagen content, followed by scaffolds seeded with 50 and 25 million cells, respectively (each $p<0.001$). The increase in collagen content was also associated with differences in cell seeding density, as collagen content normalized to DNA content was not different between groups seeded with different numbers of cells (ANOVA, $p=0.15$, Fig. 5D). This suggests that there is no significant effect of seeding density on the amount of collagen synthesized per cell.

3.4 Histology

3.4.1 Alcian blue staining—Alcian blue staining indicated GAG accumulation in the scaffolds that varied with the seeding density (Fig. 6). With increasing cell seeding density, from 25 million cells/ml (Fig 6A–C) to 50 million cells/ml (Fig 6D–F) to 100 million cells/ml (Fig 6G–I), staining was more uniform and with fewer voids. This increased histochemical staining was consistent with the biochemical assay results, which also indicated an increase in GAG content with increasing cell seeding density (Fig. 5A). Thus, at high cell seeding density, the histochemical and biochemical results indicate formation of an approximately continuous cartilaginous extracellular matrix rich in proteoglycan.

3.4.2 Immunohistochemistry—Immunohistochemical staining showed the absence of Type I collagen (Fig. 7) and the presence of Type II collagen (Fig. 8) in engineered silk cartilaginous constructs. As with histochemical staining for sulfated glycosaminoglycan, immunostaining showed increasingly contiguous and intense staining and the absence of voids as seeding density increased from 25, to 50 and 100 million cells/ml after culture for 14 days. These results are generally consistent with the biochemical analyses of the constructs (Fig. 5C).

3.5 Biomechanical Properties of Silk Fibroin-Cartilaginous Constructs

3.5.1 Static Biomechanical Properties—The static equilibrium modulus, E, varied between the non-seeded scaffolds and the seeded constructs ($p<0.05$, Fig. 9A). The non-seeded scaffold, the constructs seeded with 25 million cells per ml, and the constructs seeded with 50 million cells per ml had similarly low moduli, averaging 1.4 kPa, 1.3 kPa, and 0.9 kPa, respectively. Constructs seeded with 100 million cells per ml had a higher modulus of 6.1 kPa.

3.5.2 Dynamic Biomechanical Properties—The dynamic unconfined compression stiffness (Fig. 9B) also varied between the non-seeded and seeded constructs (ANOVA $p<0.05$) and with frequency (ANOVA $p<0.001$) with an interaction effect ($p<0.005$). At a low frequency of 0.005 Hz, trends were similar to those of equilibrium modulus, with non-seeded scaffold, the constructs seeded with 25 million cells per ml, and the constructs seeded with 50 million cells per ml had similarly low moduli, averaging 5.2 kPa, 3.9 kPa, and 4.2 kPa, respectively. In contrast, constructs seeded with 100 million cells per ml had a higher modulus of 42.5 kPa. At a frequency of 1.5 Hz, the dynamic stiffness of the non-seeded scaffold, the constructs seeded with 25 million cells per ml, and the constructs seeded with 50 million cells/ml were similar, averaging 8 kPa, 12 kPa, and 22 kPa, respectively, whereas constructs seeded with 100 million cells/ml had a higher modulus of 107 kPa.

The phase angle of dynamic stiffness also indicated distinct differences dynamic behaviour (Fig. 9C), with differences between the non-seeded scaffolds and seeded constructs (ANOVA $p<0.05$) and with frequency (ANOVA $p<0.001$) with an interaction effect ($p<0.001$). Non-seeded constructs and scaffolds seeded with 25 million cell/ml or 50 million cells/ml had similar trends of generally increasing phase shift with increasing test frequency from f=0.005 Hz to f=1.5 Hz, ranging from 10–20 degrees for non-seeded scaffolds to 18–34 degrees and 24–39 degrees for constructs seeded with 25 million cell/ml or 50 million cells/ml, respectively. However, the phase angle of samples seeded with 100 million cells per ml decreased from 39 to 28 degrees over the same test frequency sweep.

3.6 Composition–structure–function relationships

Static equilibrium compressive modulus, dynamic stiffness and dynamic stiffness phase were correlated with GAG and collagen content in the constructs. Static equilibrium

compressive modulus dynamic stiffness amplitude and dynamic stiffness phase were positively correlated to total GAG content by univariate regression (Figs. 10D–F). Static equilibrium compressive modulus was also positively correlated to collagen content by univariate regression (Fig. 10G). Similarly, multivariate regression analysis indicated that the static equilibrium modulus (R^2=0.30, Fig. 10A), dynamic stiffness amplitude (R^2=0.31, Fig. 10B) and dynamic stiffness phase were related to collagen and GAG content (R^2=0.26, Fig. 10C).

4. DISCUSSION

Tissue engineering and modelling of native articular cartilage *in vitro* requires an appropriate density and function of chondrocytes in a three-dimensional environment. The *A. mylitta* silk fibroin scaffold provided a cytocompatible, three-dimensional structure that allowed cartilaginous tissue development. The seeded scaffolds showed an increase in thickness and wet weight after 14 days of culture when compared to non seeded scaffolds of the same initial dimensions (Fig. 2)The bovine chondrocytes were able to adhere and proliferate in a dose-dependent manner and remain viable throughout the construct (Figs. 3 and 4). Also, the chondrocytes were able to synthesize and accumulate extracellular matrix typical of articular cartilage (Figs. 5–8). Additionally, there were marked effects of cell seeding on compressive biomechanical properties (Fig. 9), with a marked effect at 100 million cells/ml with such constructs having compressive moduli and stiffness 4–5× folds that of cell-free scaffolds. The biomechanical properties were correlated to the GAG and COL content. The results indicate that immature bovine chondrocytes seeded onto *A. mylitta* silk fibroin protein scaffolds may subsequently develop into cartilaginous constructs, which may alter the load-bearing, reparative and integrative capabilities in therapeutic applications *in vivo*.

The assessment of the compressive biomechanical properties of cartilage, and the analysis of the relationships between these biomechanical and biochemical properties required attention to experimental issues. The chondrocytes were not segregated into different zones of cartilage (superficial, middle and deep), but all cell types were used as a mixed population to represent the cartilage tissue as a whole. Immature knee femoral condyle chondrocytes were used for practical purpose of more cellularity and matrix content. Nutrients were made available by defining an appropriate cell density to media ratio during the culture.

A number of features of the scaffold may have been critical to the cell density-dependent development of cartilaginous tissue properties. The *A. mylitta* silk fibroin scaffolds provided a permissive microenvironment for chondrogenesis and the chondrocyte phenotype. The highly porous scaffold allowed cells to disperse throughout [19]. The attachment of cells may have been facilitated by the presence of RGD sequences in the skil fibroin and an appropriate surface morphology of the protein [40–42], as the presence of RGD can enhance chondrogenesis [43].

Higher cell density and longer culture duration were found to be associated with increased collagen and GAG content (Figs. 5–8). The collagen content of the scaffolds seeded with 100 million cells/ml was found to be highest. In both immature and adult bovine cartilage, more than 90% of collagen in cartilage is Type II [44] and more abundant staining of Type II collagen was observed in the engineered constructs. GAG normalized to the volume of scaffold is quite high for scaffolds seeded with 100 million cells/ml. The average GAG contents for 25, 50 and 100 million cells/ml seeded constructs at the end of 14 days were 9, 16 and 29 mg/ml of scaffold volume, and thus ranges from less than to more than that (15 mg/ml) in agarose plugs (initial seeding density of 20 million cells/ml) at end of 36 days [45] as well as that (25 mg/ml) of bovine cartilage [46] which has a cell density that ranges

from 150–50 million cells/ml through the depth of the tissue [47]. Hence, a significant amount of proteoglycan was synthesized in the silk fibroin-cartilaginous constructs. Also, GAG content, when normalized to DNA, provided evidence that the production of GAG is not markedly dependent upon the initial cell seeding density. Finally, a substantial proportion of GAG was retained within the scaffold (Fig. 5). This may be due to the accumulation of collagen synthesized by the cells in the scaffold and forming a mesh which entraps the proteoglycan molecules [25].

In addition, significant relationships were observed between effects of cell seeding on compressive biomechanical properties (Fig. 9) and matrix accumulation in compression (Fig. 10). Unconfined static compressive modulus and dynamic stiffness of tissue-engineered constructs varied with sulfated glycosaminoglycan (GAG) and collagen contents produced by articular chondrocytes seeded at various densities. While the equilibrium compressive modulus of the silk fibroin scaffold seeded with 100 million cells/ml was 5 fold that of the non-seeded constructs, the value of 6 kPa was less than that of native articular cartilage [48–53]. This may be due to several factors, comprising the overall matrix component and its structure. It could be due to a relatively low collagen content as the compressive properties of articular cartilage are dependent on the collagen content [46] as well as the tensile properties of the collagen–proteoglycan extracellular matrix [54–58]. The mechanical properties of these constructs could be enhanced by modifying the scaffold properties, increasing the duration of culture period, or providing additional biochemical and biomechanical stimuli [59, 60]. A more thorough analysis of these factors may provide additional insight into the mechanisms governing the formation, development and behaviour of the functional matrix in silk fibroin- cartilaginous constructs.

5. CONCLUSION

Non-mulberry tropical tasar silkworm, *Antheraea mylitta* silk fibroin protein scaffolds fabricated by freeze drying, fulfilled two major functions. First, they serve as a cytocompatible carrier for chondrocytes and can cover the hypothetical defect; second, they are designed to support the growth and proliferation of the cultivated cells for a prolonged duration. The cell seeding density had dramatic substantial effect on the biochemical and biomechanical properties of the *in vitro* cartilaginous constructs. In addition, the biomechanical properties of the construct were correlated with cell seeding density and matrix accumulation. The results have important implications for interpreting the results of chondrocyte mechanotransduction and mechanobiology studies, for developing further complex *in vitro* models of such culture systems as well as for cell-based regenerative cartilage tissue engineering.

Acknowledgments

The work was financially supported by Indo-US Science and Technology Forum (SCK, RLS), New Delhi, Department of Biotechnology (SCK and Fellowship to ST) and Department of Science and Technology (SCK), Government of India, the National Institutes of Health (RLS), and a grant to University of California-San Diego, from the Howard Hughes Medical Institute through the HHMI Professors Program (RLS). We (SCK and ST) are indebted to RLS for the support during our visits to his laboratory. We (RLS and QTN) are also grateful for our short visits to the laboratory of SCK at Indian Institute of Technology Kharagpur.

REFERNCES

1. Eggli PS, Hunziker EB, Schenk RK. Quantitation of structural features characterizing weight- and less-weight-bearing regions in articular cartilage: a stereological analysis of medial femoral condyles in young adult rabbits. Anat Rec. 1988; 222:217–27. [PubMed: 3213972]
2. Xie J, Han Z, Naito M, Maeyama A, Kim SH, Kim YH, et al. Articular cartilage tissue engineering based on a mechano-active scaffold made of poly(L-lactide-co-epsilon-caprolactone): *In vivo*

performance in adult rabbits. J Biomed Mater Res B Appl Biomater. 2010; 94:80–8. [PubMed: 20336738]

3. Göhring AR, Lübke C, Andreas K, Kaps C, Häupl T, Pruss A, et al. Tissue-engineered cartilage of porcine and human origin as *in vitro* test system in arthritis research. Biotechnol Prog. 2010; 26:1116–25. [PubMed: 20306542]
4. Frenkel SR, Di Cesare PE. Scaffolds for articular cartilage repair. Ann Biomed Eng. 2004; 32:26–34. [PubMed: 14964719]
5. Guilak F, Butler DL, Goldstein SA. Functional tissue engineering: the role of biomechanics in articular cartilage repair. Clin Orthop. 2001; 391(Suppl):S295–305. [PubMed: 11603713]
6. Hutmacher DW, Loessner D, Rizzi S, Kaplan DL, Mooney DJ, Clements JA. Can tissue engineering concepts advance tumor biology research? Trends Biotechnol. 2010; 28:125–33. [PubMed: 20056286]
7. Chaipinyo K, Oakes BW, Van Damme MP. The use of debrided human articular cartilage for autologous chondrocyte implantation: maintenance of chondrocyte differentiation and proliferation in type I collagen gels. J Orthop Res. 2004; 22:446–55. [PubMed: 15013108]
8. Grigolo B, Roseti L, Fiorini M, Fini M, Giavaresi G, Aldini N, et al. Transplantation of chondrocytes seeded on a hyaluronan derivative (hyaff-11) into cartilage defects in rabbits. Biomaterials. 2001; 22:2417–24. [PubMed: 11511039]
9. Hendrickson DA, Nixon AJ, Grande DA, Todhunter RJ, Minor RM, Erb H, et al. Chondrocyte-fibrin matrix transplants for resurfacing extensive articular cartilage defects. J Orthop Res. 1994; 12:485–96. [PubMed: 8064479]
10. Rahfoth B, Weisser J, Sternkopf F, Aigner T, von der Mark K, Brauer R. Transplantation of allograft chondrocytes embedded in agarose gel into cartilage defects of rabbits. Osteoarthritis Cartilage. 1998; 6:50–65. [PubMed: 9616439]
11. Ragetly GR, Slavik GJ, Cunningham BT, Schaeffer DJ, Griffon DJ. Cartilage tissue engineering on fibrous chitosan scaffolds produced by a replica molding technique. J Biomed Mater Res A. 2010; 93:46–55. [PubMed: 19484774]
12. Alves da Silva ML, Crawford A, Mundy JM, Correlo VM, Sol P, Bhattacharya M, et al. Chitosan/polyester-based scaffolds for cartilage tissue engineering: assessment of extracellular matrix formation. Acta Biomater. 2010; 6:1149–57. [PubMed: 19788942]
13. Müller FA, Müller L, Hofmann I, Greil P, Wenzel MM, Staudenmaier R. Cellulose-based scaffold materials for cartilage tissue engineering. Biomaterials. 2006; 27:3955–63. [PubMed: 16530823]
14. Wang Y, Bella E, Lee CS, Migliaresi C, Pelcastre L, Schwartz Z, et al. The synergistic effects of 3-D porous silk fibroin matrix scaffold properties and hydrodynamic environment in cartilage tissue regeneration. Biomaterials. 2010; 31:4672–81. [PubMed: 20303584]
15. Kawakami M, Tomita N, Shimada Y, Yamamoto K, Tamada Y, Kachi N, et al. Chondrocyte distribution and cartilage regeneration in silk fibroin sponge. Biomed Mater Eng. 2011; 21:53–61. [PubMed: 21537063]
16. Cohen SB, Meirisch CM, Wilson HA, Diduch DR. The use of absorbable co-polymer pads with alginate and cells for articular cartilage repair in rabbits. Biomaterials. 2003; 24:2653–60. [PubMed: 12726719]
17. Kang SW, Jeon O, Kim BS. Poly(lactic-co-glycolic acid) microspheres as an injectable scaffold for cartilage tissue engineering. Tissue Eng. 2005; 11:438–47. [PubMed: 15869422]
18. Wang C-Z, Ho M-L, Chen W-C, Chiu C-C, Hung Y-L, Wang C-K, et al. Characterization and enhancement of chondrogenesis in porous hyaluronic acid-modified scaffolds made of PLGA(75/25) blended with PEI-grafted PLGA(50/50). Materials Science and Engineering C. 201110.1016/j.msec.2011.04.019
19. Kemppainen JM, Hollister SJ. Tailoring the mechanical properties of 3D-designed poly(glycerol sebacate) scaffolds for cartilage applications. J Biomed Mater Res A. 2010; 94:9–18. [PubMed: 20091702]
20. Vepari C, Kaplan DL. Silk as a Biomaterial. Prog Polym Sci. 2007; 32:991–1007. [PubMed: 19543442]
21. Hardy JG, Scheibel TR. Composite materials based on silk proteins. Prog Polym Sci. 2010; 35:1093–1115.

22. Seda Tigli R, Ghosh S, Laha MM, Shevde NK, Daheron L, Gimble J, et al. Comparative chondrogenesis of human cell sources in 3D scaffolds. J Tissue Eng Regen Med. 2009; 3:348–360. [PubMed: 19382119]

23. Acharya C, Ghosh SK, Kundu SC. Silk fibroin film from non-mulberry tropical tasar silkworms: A novel substrate for *in vitro* fibroblast culture. Acta Biomater. 2009; 5:429–37. [PubMed: 18676188]

24. Mandal BB, Kundu SC. Non-bioengineered silk gland fibroin protein: characterization and evaluation of matrices for potential tissue engineering applications. Biotechnol Bioeng. 2008a; 100:1237–50. [PubMed: 18383269]

25. Mandal BB, Kundu SC. Non-bioengineered silk fibroin protein 3D scaffolds for potential biotechnological and tissue engineering applications. Macromol Biosci. 2008b; 8:807–18. [PubMed: 18702171]

26. Williams GM, Klein TJ, Sah RL. Cell density alters matrix accumulation in two distinct fractions and the mechanical integrity of alginate–chondrocyte constructs. Acta Biomater. 2005; 1:625–33. [PubMed: 16701843]

27. Revell CM, Reynolds CE, Athanasiou KA. Effects of initial cell seeding in self assembly of articular cartilage. Ann Biomed Eng. 2008; 36:1441–48. [PubMed: 18574692]

28. Buckley CT, Thorpe SD, O'Brien FJ, Robinson AJ, Kelly DJ. The effect of concentration, thermal history and cell seeding density on the initial mechanical properties of agarose hydrogels. J Mech Behav Biomed Mater. 2009; 2:512–21. [PubMed: 19627858]

29. Francioli SE, Candrian C, Martin K, Heberer M, Martin I, Barbero A. Effect of three-dimensional expansion and cell seeding density on the cartilage-forming capacity of human articular chondrocytes in type II collagen sponges. J Biomed Mater Res A. 2010; 95:924–31. [PubMed: 20845491]

30. Almarza AJ, Athanasiou KA. Effects of initial cell seeding density for the tissue engineering of the temporomandibular joint disc. Ann Biomed Eng. 2005; 33:943–50. [PubMed: 16060535]

31. Concaro S, Nicklasson E, Ellowsson L, Lindahl A, Brittberg M, Gatenholm P. Effect of cell seeding concentration on the quality of tissue engineered constructs loaded with adult human articular chondrocytes. J Tissue Eng Regen Med. 2008; 2:14–21. [PubMed: 18265427]

32. Kobayashi S, Meir A, Urban J. Effect of cell density on the rate of glycosaminoglycan accumulation by disc and cartilage cells *in vitro*. J Orthop Res. 2008; 26:493–503. [PubMed: 17985391]

33. Mandal BB, Kundu SC. Osteogenic and adipogenic differentiation of rat bone marrow cells on non-mulberry and mulberry silk gland fibroin 3D scaffolds. Biomaterials. 2009; 30:5019–30. [PubMed: 19577292]

34. Klein TJ, Schumacher BL, Schmidt TA, Li KW, Voegtline MS, Masuda K, et al. Tissue engineering of stratified articular cartilage from chondrocyte subpopulations. Osteoarthritis Cartilage. 2003; 11:595–602. [PubMed: 12880582]

35. Farndale RW, Buttle DJ, Barrett AJ. Improved quantitation and discrimination of sulphated glycosaminoglycans by use of dimethylmethylene blue. Biochim Biophys Acta. 1986; 883:173–7. [PubMed: 3091074]

36. Woessner JF. The determination of hydroxyproline in tissue and protein samples containing small proportions of this amino acid. Arch Biochem Biophys. 1961; 93:440–47. [PubMed: 13786180]

37. McGowan KB, Kurtis MS, Lottman LM, Watson D, Sah RL. Biochemical quantification of DNA in human articular and septal cartilage using PicoGreen and Hoechst 33258. Osteoarthritis Cartilage. 2002; 10:580–87. [PubMed: 12127839]

38. Pal S, Tang LH, Choi H, Habermann E, Rosenberg L, Roughley P, et al. Structural changes during development in bovine fetal epiphyseal cartilage. Collagen Rel Res. 1981; 1:151–76.

39. Kim YJ, Sah RL, Doong JY, Grodzinsky AJ. Fluorometric assay of DNA in cartilage explants using Hoechst 33258. Anal Biochem. 1988; 174:168–76. [PubMed: 2464289]

40. Datta A, Ghosh AK, Kundu SC. Differential expression of the fibroin gene in developmental stages of silkworm, *Antheraea mylitta* (Saturniidae). Comp Biochem Physiol B. 2001; 129:197–204. [PubMed: 11337263]

41. Mandal BB, Das S, Chaudhury K, Kundu SC. Implication of silk film RGD availability and surface roughness on cytoskeletal organization and proliferation of primary rat bone marrow cells. Tissue Eng Part A. 2010; 16:2391–403. [PubMed: 20214452]
42. Talukdar S, Mandal M, Hutmacher DW, Russell PJ, Soekmadji C, Kundu SC. Engineered silk fibroin protein 3D matrices for *in vitro* tumor model. Biomaterials. 2011; 32:2149–159. [PubMed: 21167597]
43. Hsu SH, Huang TB, Cheng SJ, Weng SY, Tsai CL, Tseng CS, et al. Chondrogenesis from human placenta-derived mesenchymal stem cells in three-dimensional scaffolds for cartilage tissue engineering. Tissue Eng Part A. 2011; 17:1549–60. [PubMed: 21284540]
44. Williamson AK, Chen AC, Masuda K, Thonar EJ, Sah RL. Tensile mechanical properties of bovine articular cartilage: variations with growth and relationships to collagen network components. J Orthop Res. 2003; 21:872–80. [PubMed: 12919876]
45. Buschmann MD, Gluzband YA, Grodzinsky AJ, Kimura JH, Hunziker EB. Chondrocytes in agarose culture synthesize a mechanically functional extracellular matrix. J Orthop Res. 1992; 10:745–58. [PubMed: 1403287]
46. Williamson AK, Chen AC, Sah RL. Compressive properties and function-composition relationships of developing bovine articular cartilage. J Orthop Res. 2001; 19:1113–21. [PubMed: 11781013]
47. Jadin KD, Wong BL, Bae WC, Li KW, Williamson AK, Schumacher BL, et al. Depth-varying density and organization of chondrocytes in immature and mature bovine articular cartilage assessed by 3D imaging and analysis. J Histochem Cytochem. 2005; 53:1109–19. [PubMed: 15879579]
48. Armstrong CG, Mow VC. Variations in the intrinsic mechanical properties of human articular cartilage with age, degeneration, and water content. J Bone Joint Surg Am. 1982; 64:88–94. [PubMed: 7054208]
49. Buschmann MD, Kim YJ, Wong M, Frank E, Hunziker EB, Grodzinsky AJ. Stimulation of aggrecan synthesis in cartilage explants by cyclic loading is localized to regions of high interstitial fluid flow. Arch Biochem Biophys. 1999; 366:1–7. [PubMed: 10334856]
50. Sah RL, Kim YJ, Doong JY, Grodzinsky AJ, Plaas AH, Sandy JD. Biosynthetic response of cartilage explants to dynamic compression. J Orthop Res. 1989; 7:619–36. [PubMed: 2760736]
51. Kim YJ, Bonassar LJ, Grodzinsky AJ. The role of cartilage streaming potential, fluid flow and pressure in the stimulation of chondrocyte biosynthesis during dynamic compression. J Biomech. 1995; 28:1055–66. [PubMed: 7559675]
52. Ahmed AM, Burke DL. *In vitro* measurement of static pressure distribution in synovial joints—part I: tibial surface of the knee. J Biomech Eng. 1983; 105:216–25. [PubMed: 6688842]
53. Brown TD, Shaw DT. *In vitro* contact stress distributions in the natural human hip. J Biomech. 1983; 16:373–84. [PubMed: 6619156]
54. Huang CY, Mow VC, Ateshian GA. The role of flow-independent viscoelasticity in the biphasic tensile and compressive responses of articular cartilage. J Biomech Eng. 2001; 123:410–7. [PubMed: 11601725]
55. Cohen B, Lai WM, Mow VC. A transversely isotropic biphasic model for unconfined compression of growth plate and chondroepiphysis. J Biomech Eng. 1998; 120:491–6. [PubMed: 10412420]
56. Mizrahi J, Maroudas A, Lanir Y, Ziv I, Webber TJ. The —instantaneous deformation of cartilage: effects of collagen fiber orientation and osmotic stress. Biorheology. 1986; 23:311–30. [PubMed: 3779058]
57. Soltz MA, Ateshian GA. A conewise linear elasticity mixture model for the analysis of tension–compression nonlinearity in articular cartilage. J Biomech Eng. 2000; 122:576–86. [PubMed: 11192377]
58. Soulhat J, Buschmann MD, Shirazi-Adl A. A fibril- network-reinforced biphasic model of cartilage in unconfined compression. J Biomech Eng. 1999; 121:340–7. [PubMed: 10396701]
59. van der Kraan PM, Buma P, van Kuppevelt T, van den Berg WB. Interaction of chondrocytes, extracellular matrix and growth factors: relevance for articular cartilage tissue engineering. Osteoarthritis Cartilage. 2002; 10:631–7. [PubMed: 12479385]

60. Guilak F, Butler DL, Goldstein SA. Functional tissue engineering: the role of biomechanics in articular cartilage repair. Clin Orthop. 2001; 391(Suppl):S295–305. [PubMed: 11603713]

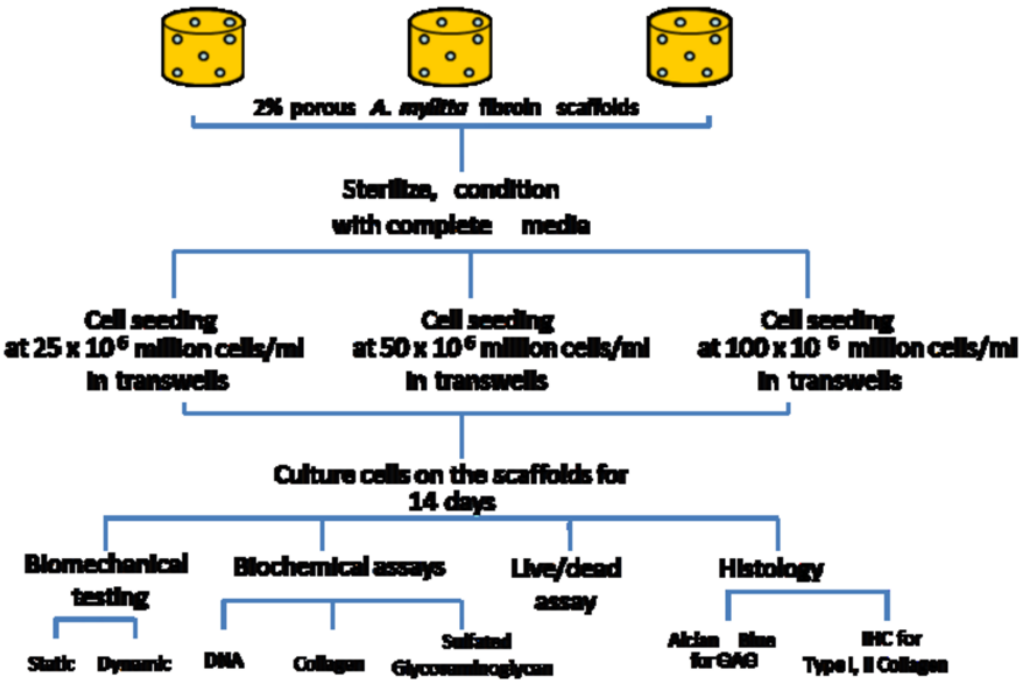

Figure 1.
A schematic representation of the procedures followed for the development of silk fibroin protein scaffolds, cell seeding, and analysis of the silk-fibroin cartilaginous constructs.

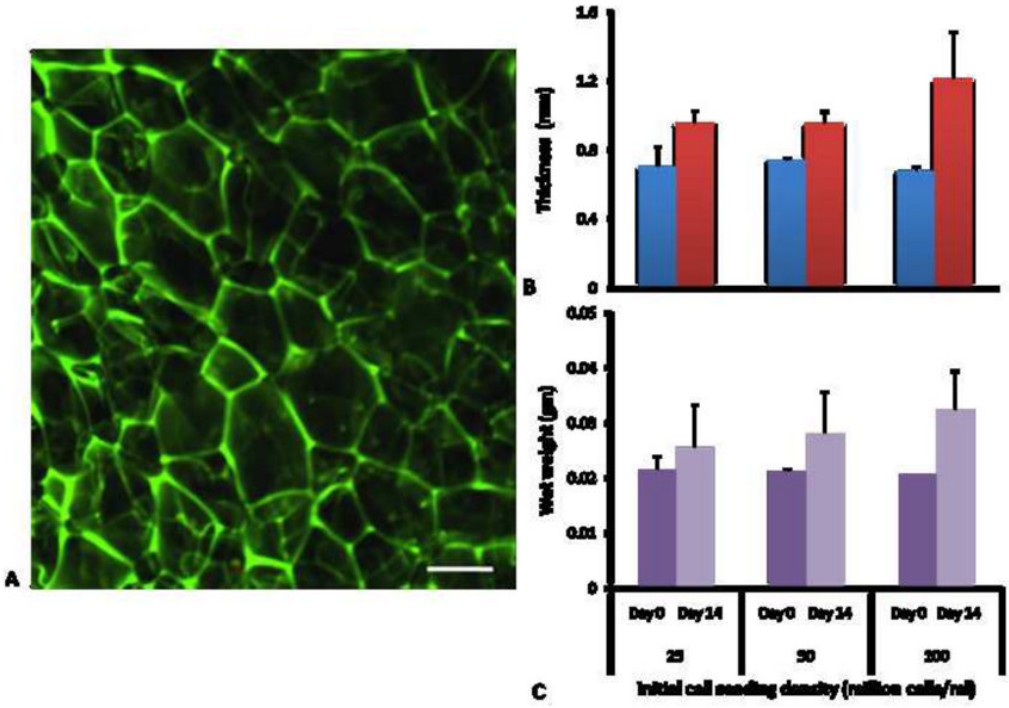

Figure 2.

A) Confocal micrograph of non-mulberry silk gland fibroin scaffold. Scale bar represents 100 μm. B) Thickness of scaffolds at Day 0 (before seeding) and Day 14 of culture (n=3–6). C) Wet weight of scaffolds at Day 0 (before seeding) and Day 14 of culture (n=3–6). Data are mean±SEM.

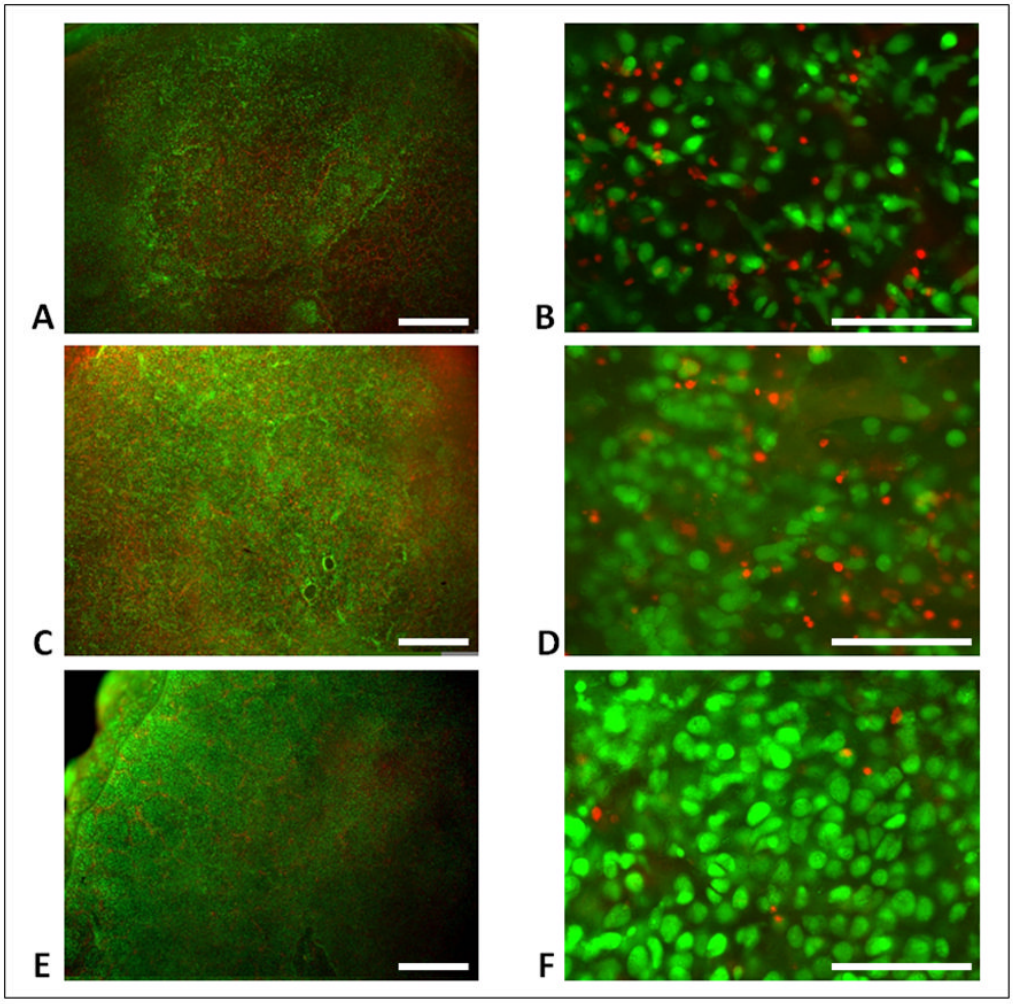

Figure 3.
Pictographs of live/dead staining of scaffolds with initial seeding of (**A, B**) 25 million cells/ml, (**C, D**) 50 million cells/ml, or (**E, F**) 100 million cells/ml. Scale bars are 500 μm (**A, C, E**) and 100 μm (**B, D, F**).

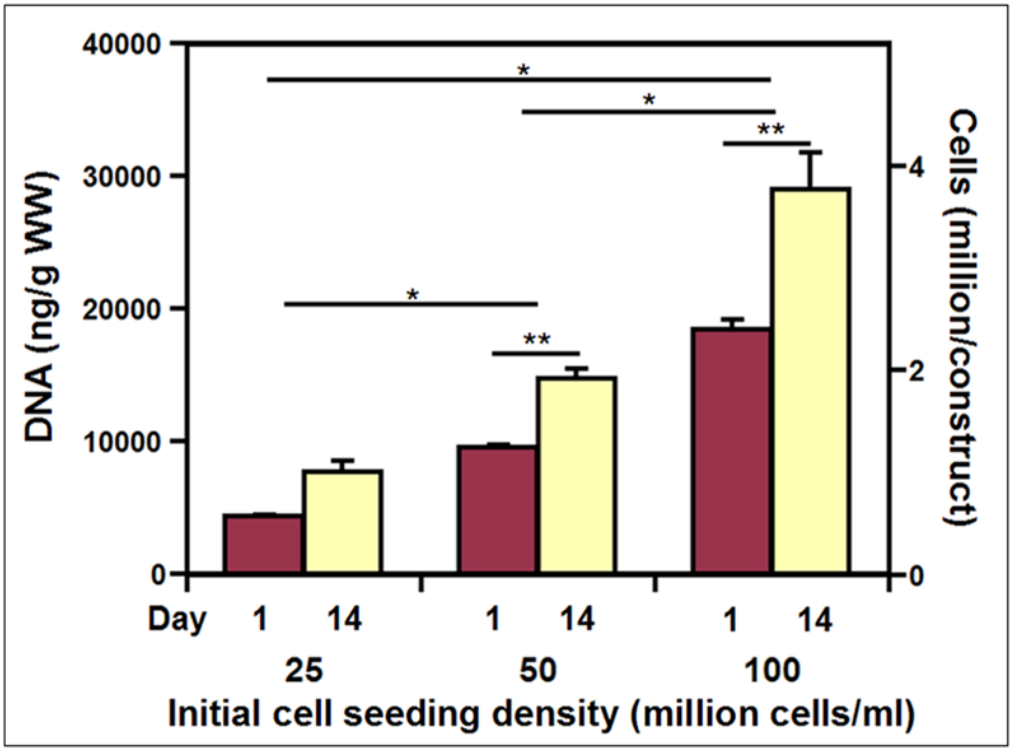

Figure 4.
Cell and DNA content of silk cartilaginous constructs at day 1 and 14 with seeding densities of 25, 50 and 100 million cells/ml. Data are mean±SEM. (n=3–6) * denotes significant difference between seeding density groups, and ** denotes significance between day 1 and 14 within groups ($p<0.05$).

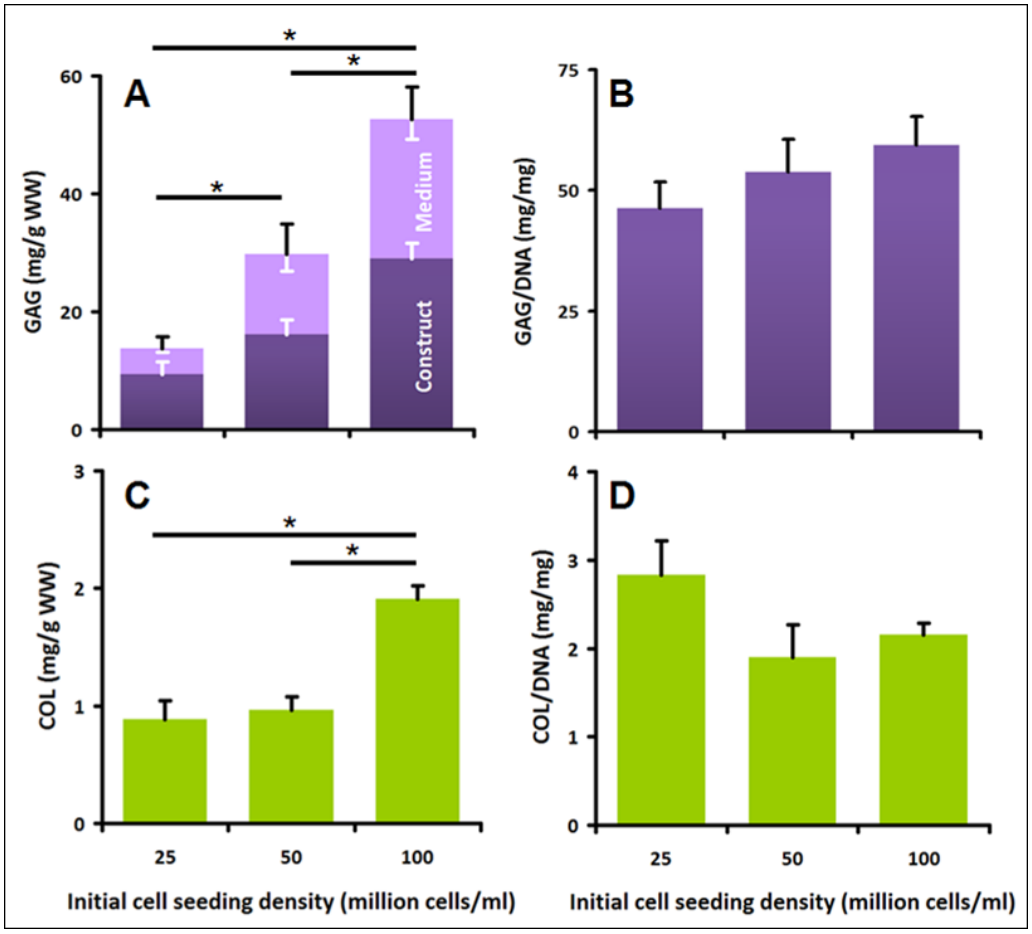

Figure 5.

Effect of cell seeding densities (25, 50 and 100 million cells/ml) on biochemical properties of constructs after 14 days of culture. A) Sulfated GAG content in construct and medium, normalized to wet weight of constructs. B) Total GAG/DNA ratio. C) Collagen content of constructs. D) Construct collagen/DNA ratio. Data are mean±SEM, white error bars for construct and medium, black error bars for overall. * indicates significance between groups ($p<0.001$).

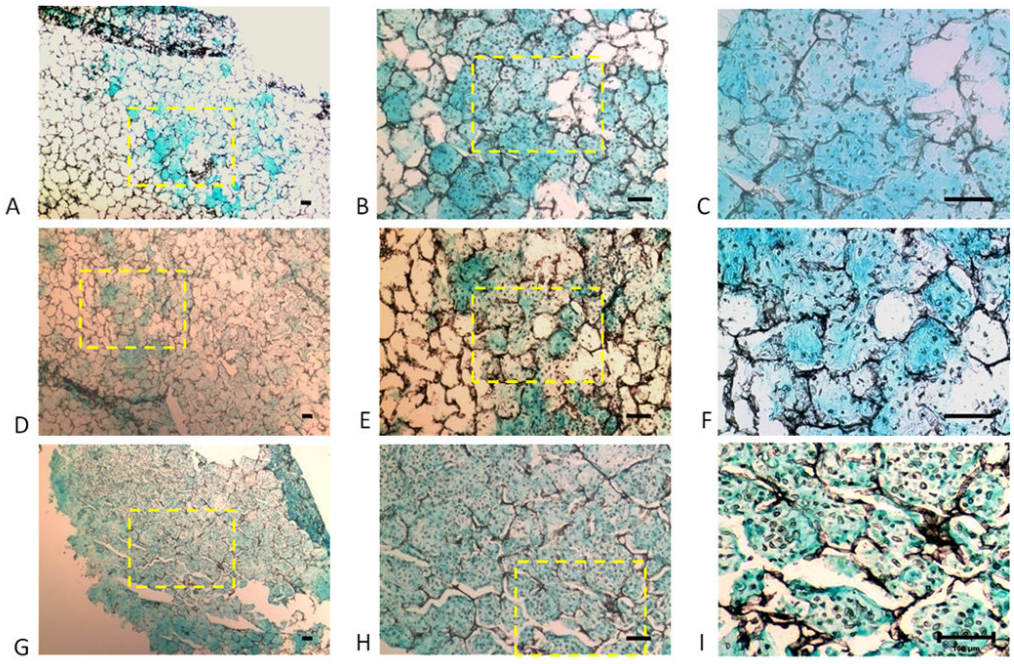

Figure 6.

Accumulation of sulfated glycosaminoglycan in engineered silk cartilaginous constructs: Photomicrographs of silk scaffolds seeded at densities of (A–C) 25; (D–F) 50; and (G–I) 100 million cells/ml after 14 days of culture after staining with Alcian Blue. With increasing seeding density, there are fewer non-stained void regions. Yellow box indicates region of higher magnification. Scale bars represent 100μm.

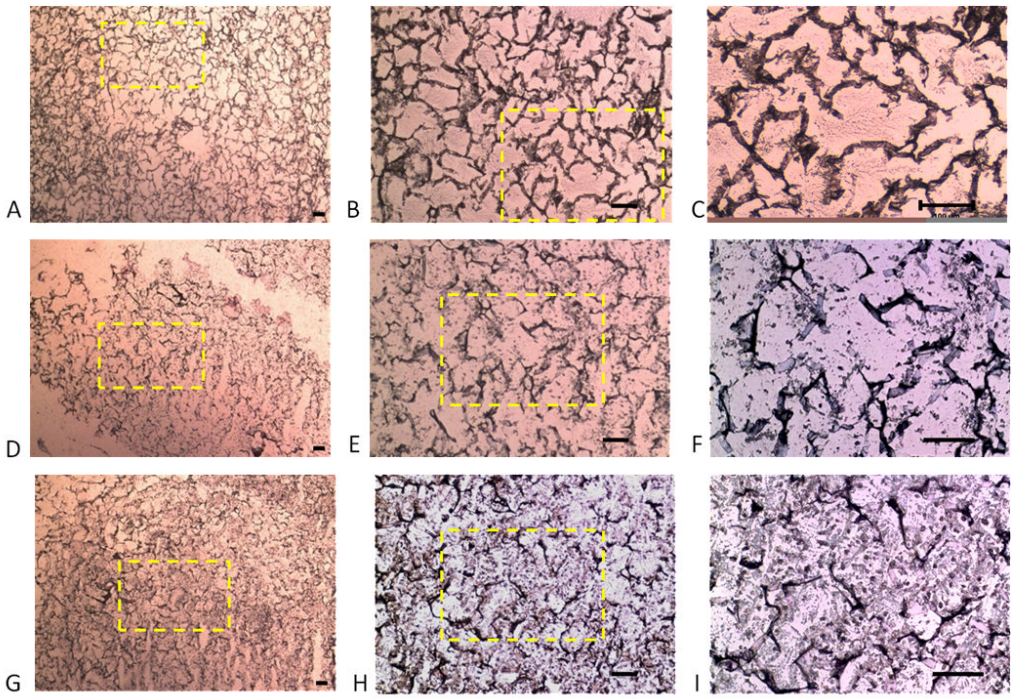

Figure 7.
Immunolocalization of Type I collagen in silk scaffolds. The scaffolds show positive immunohistochemical staining for Type I collagen (A–I) showing ample extracellular matrix formation. The initial seeding densities were 25 million cells/ml (A–C), 50 million cells/ml (D–F) and 100 million cells/ml (G–I). Yellow box indicates region of higher magnification. Scale bars represent 100μm.

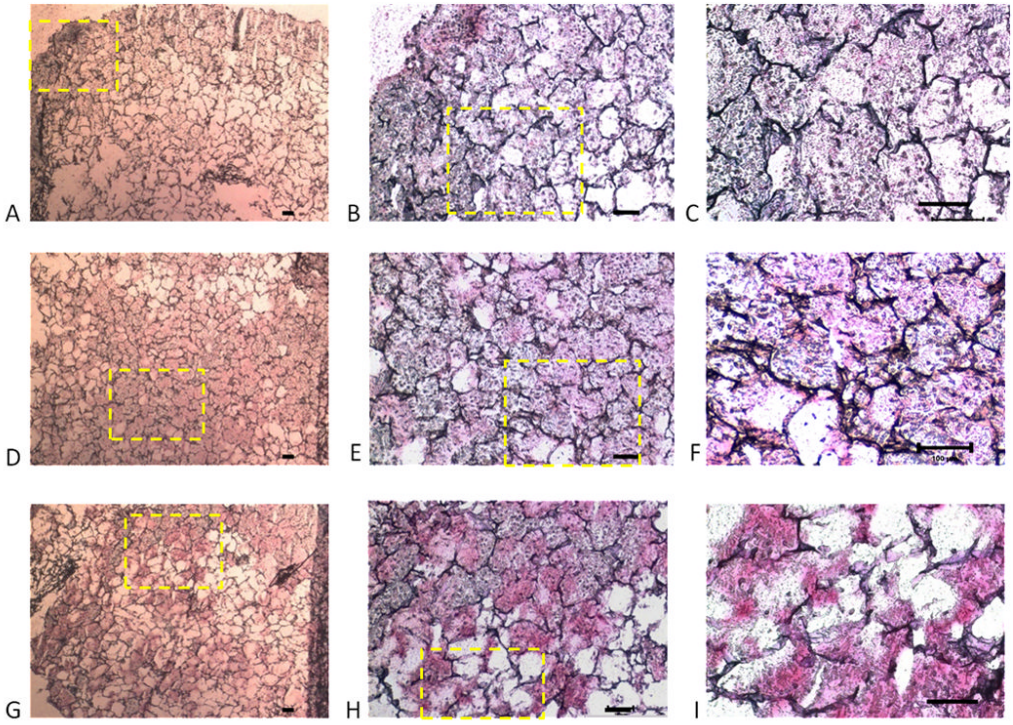

Figure 8.
Immunolocalization of Type II collagen in silk scaffolds. The scaffolds show positive immunohistochemical staining for Type II collagen showing ample extracellular matrix formation. The initial seeding densities were (A–C) 25 million cells/ml (D–F); 50 million cells/ml (G–I) and 100 million cells/ml. Yellow box indicates region of higher magnification. Scale bars represent 100μm.

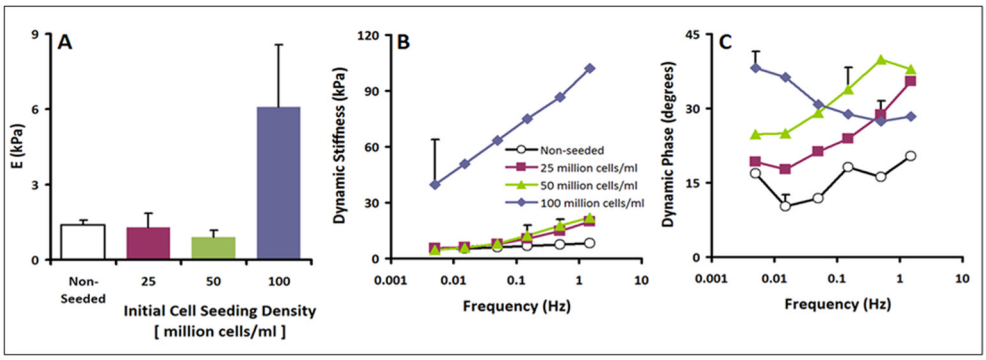

Figure 9.

Biomechanical analysis of non-seeded and scaffolds seeded with 25, 50 and 100 million cells/ml. (A) Static equilibrium modulus; (B) Dynamic Stiffness Amplitude; and (C) Phase of scaffolds (n=2–6). Data are mean±SEM. Error bars in panel B and C are averages over all test frequencies.

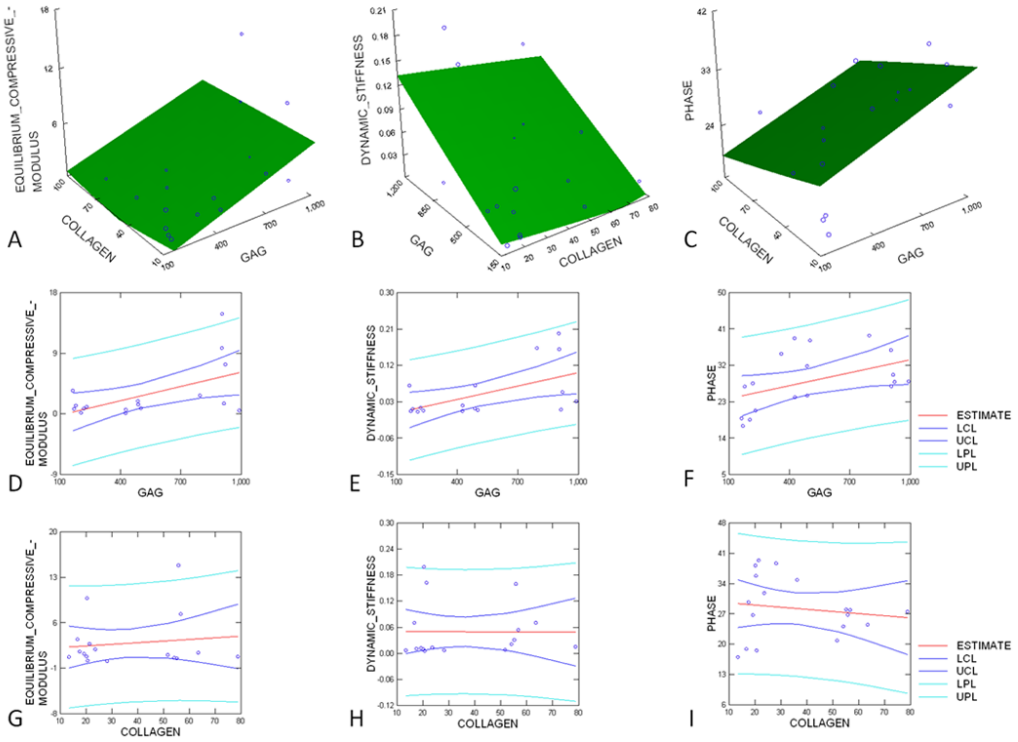

Figure 10.

Regression analysis between biomechanical and biochemical properties of the silk fibroin-cartilage constructs **(A–C):** Multiple regression analysis between the measures of A) Equilibrium compression modulus (R^2=0.30, p=0.08), B) dynamic stiffness amplitude (R^2=0.31, p=0.08) and C) dynamic stiffness phase (R^2= 0.26, p= 0.11) and biochemical content. **(D–I)**: Regression analysis between (D) static equilibrium compression modulus and GAG content (R^2=0.30, p<0.05); (E) dynamic stiffness amplitude and GAG content (R^2=0.30, p<0.05); (F) dynamic stiffness phase and GAG content (R^2=0.02, p=0.54); (G) static equilibrium compression modulus and collagen content (R^2=0.02, p=0.62); (H) dynamic stiffness and collagen content (R^2=0.00, p=0.98); (I) dynamic stiffness phase and collagen content (R^2=0.02, p=0.57). Data points are shown for constructs with initial cell densities of 25, 50 and 100 million cells/ml after 2 weeks of culture.